Model calculation for energy loss in ion-surface collisions

J. E. Miraglia and M. S. Gravielle

Instituto de Astronomía y Física del Espacio, Consejo Nacional de Investigaciones Científicas y Técnicas, Departamento de Física, Facultad de Ciencias Exactas y Naturales, Universidad de Buenos Aires, Casilla de Correo 67, Sucursal 28, 1428 Buenos Aires, Argentina

(Received 28 January 2003; published 3 June 2003)

The so-called local plasma approximation is generalized to deal with projectiles colliding with surfaces of amorphous solids and with a specific crystalline structure (plannar channeling). Energy loss of protons grazingly colliding with aluminum, SnTe alloy, and LiF surfaces is investigated. The calculations agree quite well with previous theoretical results and explain the experimental findings of energy loss for aluminum and SnTe alloy, but they fall short to explain the data for LiF surfaces.

DOI: 10.1103/PhysRevA.67.062901 PACS number(s): 34.50.Bw, 79.20.Rf, 71.10.Ca

I. INTRODUCTION

We consider here the energy loss of fast heavy projectiles grazingly colliding with solid surfaces [1]. The more rigorous approach to tackle this problem would be the determination of the so-called density response function $\varkappa(\mathbf{r},\mathbf{r}',\omega)$ for the slab, which is very time demanding in terms of computations. Instead, the most common approach consists in resorting to the basic knowledge of atomic collisions and calculating all the possible semiclassical inelastic amplitudes (excitation and ionization) in terms of the projectile impact parameters. If we employ a distorted-wave method, for example, the quantum *T*-matrix element in terms of the projectile momentum transfer is obtained instead. In this case, one should transform the quantum *T*-matrix element into the semiclassical amplitudes via the eikonal approximation. It requires a two-dimensional numerical integral for every electron energy transferred ω. It follows a numerical average over the density of atom targets of the surface to obtain the basic expression, i.e., the energy-loss distribution $dP/d\omega$ as a function of the distance of the projectile to surface Z_0. To calculate the total-energy loss, two more numerical integrations follow: on the energy loss ω and on the projectile trajectory involving all the values of Z_0. The work of Juaristi *et al.* [2] follows all these steps. When the target surface is composed of heavy atoms, such as SnTe alloys this procedure becomes extremely tedious. The main numerical task is not the treatment of the valence electrons, which can be fairly approximated by a free electron gas (FEG), but the bound electrons (BE) of the atoms composing the surface target. By BE we refer to the atomic description we use; not necessarily to inner shells but also to states with negative energies (the electrons of the $F^-(2p)$ state, for example, will be here considered BE).

In this work we start from a simple model describing the interaction of projectiles with BE of many-electron atoms that is the local plasma approximation (LPA) [3,4]. One expects that the more electrons the target atom has, the better the LPA will be. The LPA describes quite well the case of projectiles moving in the *bulk*, i.e., inside the solid in the perturbative regime [5–7]. Results using the LPA approximation were reported recently for impact of protons on different solids such as aluminum, copper, and silicon [5]; the mean free path, the stopping, and the straggling were compared with the experiments and the agreement was excellent.

Our goal here is to extend the LPA to deal with grazing collisions with *surfaces*. We put forward two approaches. First, we propose a model developed to deal with FEG edges, the so-called axial model (AM) [8]. The AM intends to be a much simpler but still precise version of the so-called specular reflection model (SRM) [9–12]. We expect the AM to describe surfaces of amorphous solids, i.e., noncrystalline surfaces. Our second proposal deals with crystalline surfaces. To that end, we reformulate the LPA to yield an expression that we call the surface local plasma approximation (SLPA), which accounts for planar channeling. This approximation, as we will prove, explains quite well the results of Juaristi *et al.* [2] and the experiments with conductor surfaces, but not the LiF case. Atomic units are used unless otherwise stated.

II. THEORY

A. Dielectric formalism at surfaces

We are interested in studying the process of projectiles moving parallel to the surface, instead of moving well inside the solid [8,13,14]. The relevant quantity to describe the energy-loss distribution of a projectile interacting with the valence electrons at the surface is introduced as a straight *generalization* of the dielectric response function. It is here denoted with $\varepsilon(q,\omega,Z_0)$, where q is the momentum transfer, ω is the energy deposited, and Z_0 is the distance of the projectile to the surface. The energy and momentum-loss spectrum $d^2P(Z_0)/d\omega dq$ per unit path is related to $\varepsilon(q,\omega,Z_0)$ in the usual way

$$\frac{d^2P(Z_0)}{d\omega dq}=\frac{S_0}{q}\,\mathrm{Im}\left[\frac{1}{\varepsilon(q,\omega,Z_0)}\right], \tag{1}$$

with $S_0=-2Z_P^2/(\pi v^2)$, and the moments of the energy loss can be written then as

$$P^{(n)}(Z_0)=\int_0^\infty d\omega\,\omega^n\int_{\omega/v}^\infty dq\,\frac{d^2P(Z_0)}{d\omega dq}, \tag{2}$$

where $n=0$ corresponds to the probability [or the inverse of the mean free path, $\Lambda(Z_0)=1/P^{(0)}(Z_0)$], $n=1$ to the stopping, $P^{(1)}(Z_0)=S(Z_0)$, and $n=2$ to the straggling $P^{(2)}(Z_0)=\Omega^2(Z_0)$.

Deep inside an amorphous solid (atoms at random), we should find that $\varepsilon(q,\omega,Z_0)\to\varepsilon(q,\omega)$, as $Z_0\to-\infty$, $\varepsilon(q,\omega)$ being the usual dielectric function. In case of dealing with valence electrons, they are generally described as a FEG and therefore the Lindhard [random-phase approximation (RPA)] dielectric function $\varepsilon_L(q,\omega)$ is used [15].

B. Interaction with the FEG

One of the more popular models to describe inelastic precesses with the FEG in the presence of surfaces is the SRM. This model allows us to describe the electron-loss distribution knowing the bulk dielectric function $\varepsilon(q,\omega)$ [9–12]. In a recent paper, another approximation for the dielectric function—called AM—was proposed and explored in detail [8]. By comparing the mean free path, stopping, straggling, and the induced potential, it was found that there is no appreciable difference between the AM and the SRM for proton impact energies ranging from keVs to MeVs. Moreover, there are a number of advantages of the AM, such as a simple closed form and a straight separation between binary and collective modes. In essence, the AM keeps the simplicity of the bulk expression, and the expression to be used in Eq. (1) reads [8]

$$\frac{1}{\varepsilon_{AM}(q,\omega,Z_0)}=[1+R(q,\omega)E(q'_\parallel)]\Theta(Z_0)+[1-R(q,\omega)E(q'_\parallel)]\frac{1}{\varepsilon(q,\omega)}\Theta(-Z_0), \tag{3}$$

with $E(q'_\parallel)=\exp(-2q'_\parallel|Z_0|)$, $q'_\parallel=\sqrt{(q^2+\omega^2/v^2)/2}$,

$$R(q,\omega)=\frac{1-\varepsilon(q,\omega)}{1+\varepsilon(q,\omega)}, \tag{4}$$

and Θ is the Heaviside function. In Eqs. (3) and (4), $\varepsilon(q,\omega)$ is the dielectric response function of the FEG, namely, $\varepsilon_L(q,\omega)$. In Ref. [8], the Mermin-Lindhard dielectric function was used instead, to account for plasmon decay lifetime [16].

C. Interaction with the BE

1. Random scattering

The AM was designed to deal with a projectile moving parallel to the surface, interacting with a FEG. We here extend the AM to deal with BE of surface atoms by simply using the same equations, given by Eqs. (3) and (4) but replacing $\varepsilon(q,\omega)$ by the LPA dielectric response function $\varepsilon_{LPA}(q,\omega)$, accounting for the BE instead of the FEG.

In case of dealing with BE of the solid atoms in the bulk, the dielectric function $\varepsilon_{LPA}(q,\omega)$ is defined as [3–7]

$$\frac{1}{\varepsilon_{LPA}(q,\omega)}=\frac{1}{V_{WS}}\int d\mathbf{r}\,\frac{\Theta(R_{WS}-r)}{\varepsilon_L(q,\omega,k_F(r))}, \tag{5}$$

where $V_{WS}=4/3\pi R_{WS}^3$, $R_{WS}=(3/4\pi\delta_V)^{1/3}$ is the Wigner-Seitz sphere radius, δ_V is the volume density of atoms, $k_F(r)=[3\pi^2 n(r)]^{1/3}$ is the local Fermi velocity, and $n(r)$ is the electronic local density of the bound state. In Eq. (5) $\varepsilon_L(q,\omega,k_F)$ is the RPA or Lindhard dielectric response function (we will omit variable k_F when possible).

The expression given by Eq. (5) could be called the *restricted* form used in solids. Alternatively, if we are interested in collisions with isolate atoms in a gas phase, the cross section per atom is defined as $\sigma^{(n)}=P^{(n)}V_{WS}$ and $\Theta(R_{WS}-r)$ is removed from Eq. (5), giving rise to the *unrestricted* form. As the mean radius of the BE considered is much smaller than R_{WS}, both results, the restricted and unrestricted, are equal.

In case of dealing with BE of the solid atoms in the surface, the surface edge needs to be determined. In the case of a FEG, the edge is commonly shifted half of the planar atom separation from the topmost atomic plane. For BE states, we follow an equivalent approach, i.e., the BE edge is shifted a quantity equal to the radius of the bound state considered. The extension of the AM to account for BE is only applicable when we are in the presence of a surface of an amorphous solid, more specifically when the atoms are at random. This is so because in Eq. (5) all the values of r (the distance of the projectile to the target nucleus) are permitted. This is not the case of most experiments, where the surface is determined by a specific crystalline plane and not all the values of r are permitted.

2. Planar channeling scattering

As we deal with a specific crystalline surface, we can no longer use the AM, since we are at planar channeling conditions. The approximation that we will follow here is an extension of the LPA to deal with collisions with localized states at a given crystallographic plane. If we are interested in the impact-parameter dependence of the cross section per atom $\sigma^{(0)}=P^{(0)}V_{WS}$, it results from Eq. (5) after writing $d\mathbf{r}=d\mathbf{b}dx$ [7],

$$\frac{d^4\sigma^{(0)}}{d\mathbf{b}d\omega dq}(b)=\frac{S_0}{q}\,\mathrm{Im}\left[\frac{1}{\varepsilon'_L(q,\omega,b)}\right], \tag{6}$$

$$\frac{1}{\varepsilon'_L(q,\omega,b)}=\int_{-\infty}^{\infty}dx\,\frac{1}{\varepsilon_L(q,\omega,k_F(r))}, \tag{7}$$

where b is the impact parameter and $r=\sqrt{b^2+x^2}$. Next we can write the double differential probability per unit path at a given distance to surface Z_0, in its usual form

$$\frac{d^2P}{d\omega dq}(Z_0)=\delta_s\int_{-\infty}^{\infty}dy\,\frac{d^4P}{d\mathbf{b}d\omega dq}(b=\sqrt{Z_0^2+y^2}), \tag{8}$$

where δ_S is the surface density of atoms, $\delta_S=1/S_{WS}$, and $S_{WS}=\pi\rho_{WS}^2$. Replacing Eq. (6) in Eq. (8) and introducing polar coordinates $dxdy=d\rho=\rho\,d\rho d\phi$, we arrive at an expression similar to Eq. (1),

$$\frac{d^2P}{d\omega dq}(Z_0)=\frac{S_0}{q}\,\mathrm{Im}\left[\frac{1}{\varepsilon_{SLPA}(q,\omega,Z_0)}\right], \tag{9}$$

where now

$$\frac{1}{\varepsilon_{SLPA}(q,\omega,Z_0)}=\frac{1}{S_{WS}}\int d\rho\,\frac{\Theta(\rho_{WS}-\sqrt{Z_0^2+\rho^2})}{\varepsilon_L(q,\omega,k_F(Z_0,\rho))}, \tag{10}$$

$$k_F(Z_0,\rho)=[3\pi^2 n(r=\sqrt{Z_0^2+\rho^2})]^{1/3}, \tag{11}$$

is the local Fermi velocity, and $n(r)$ is again the electronic local density of the bound states. As the atoms have azimuthal symmetry, we can write $d\rho=2\pi\rho d\rho$ and Eq. (10) can be reduced to a one-dimensional numerical integral.

Based on its volume definitions, as given by Eq. (5), $\varepsilon_{LPA}(q,\omega,k_F(r))$ requires an average of all possible projectile distances to the nucleus of a sphere of radius r. It becomes then natural that, when dealing with planar channeling, one should average all the positions of the projectile at distances Z_0 to the surface. In Eq. (10) we have explicitly included $\Theta(\rho_{WS}-\sqrt{Z_0^2+\rho^2})$ and so it should be named the *restricted* form. Similarly, one can write the *unrestricted* form by excluding such a constrain in the integrand of Eq. (10). Note that the circle of polar radius ρ_{WS}, and not the sphere of radius R_{WS}, represents the actual density of atoms crossed by the projectile at planar channeling conditions.

Before proceeding, we would like to note a straightforward extension of the LPA as explained next. As the projectile moves inside the solid, the LPA is expressed in terms of a *volume* integral, Eq. (5), while for projectiles moving parallel to a surface, the SLPA is expressed in terms of a surface integral, Eq. (10). One can then expect that for projectiles moving along a specific path in relation to the lattice (axial channeling for example), the LPA can be simply generalized to a *linear* integral along its trajectory.

III. COMPARISON WITH OTHER THEORETICAL MODELS

We will concentrate on protons moving parallel to aluminum and LiF surfaces. In all the cases, the restricted form of the LPA was used.

A. Energy loss from aluminum

Stoppings per unit path length of 700- and 1500-keV protons on aluminum (111) surfaces are shown in Fig. 1 as a function of Z_0 due only to the BE $(2s+2p)$. Also in that figure, we display our AM (dotted line) and SLPA (solid lines) predictions along with the results of Juaristi *et al.* [2], obtained using the first Born approximation. To represent the BE states, we have employed the Hartree-Fok multiple z functions given by Bunge *et al.* [17]. The Al(111) atomic density produces $\rho_{WS}=2.83$, not very different from $R_{WS}=2.98$. The shift of the edges with respect to the atomic surface when using the AM was: $(1/\delta)^{1/3}/2=2.4$ for the FEG, 0.60 for the $2p$, and 0.62 for the $2s$ bound states [17]. For the SLPA there is no need to shift the BE edges. The contribution of the inner shell $1s$ was neglected. The numerical task requires just a three-dimensional integral on $r(\rho)$, q, and ω to calculate the present results for the AM (SLPA).

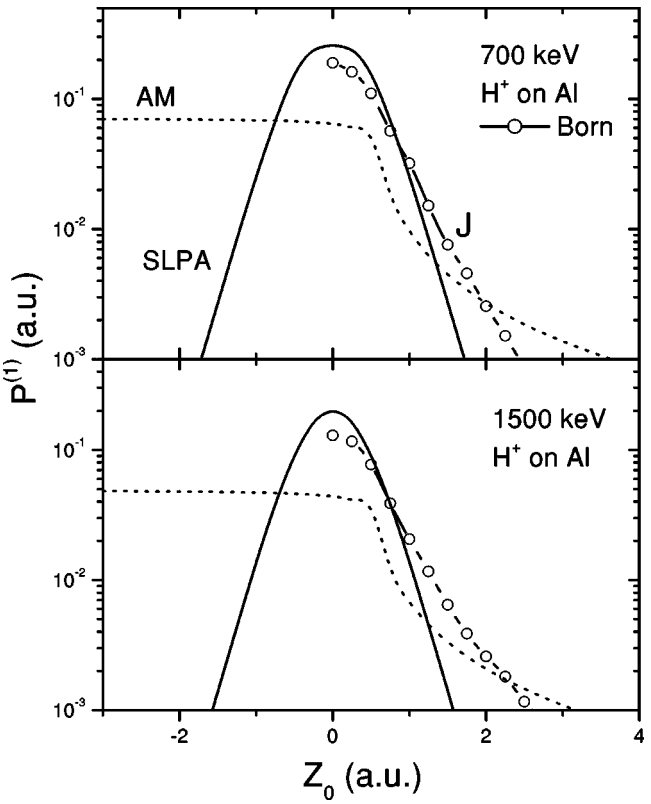

FIG. 1. Proton energy loss per unit length due to the bound electron states $(2s+2p)$ of aluminum as a function of the distance to the atomic plane. Impact proton energies as indicated. Notation: line plus empty circles, denoted *J*, results of Juaristi *et al.* [2] using the first Born approximation; dotted lines, the axial model results; and solid lines, surface local plasma approximation.

As the projectile travels into the solid $(Z_0\rightarrow-\infty)$, the stopping predicted by the AM due to the bound states $(2p+2s)$ tends to the value 0.070 (0.048) for 700 (1500) keV, which coincides quite well with the results obtained with the first Born approximation 0.058 (0.048) and the continuum distorted-wave eikonal initial state (CDW-EIS) 0.055 (0.037) within the solid. If we add the contribution of the FEG we have a total stopping, which is very near the experimental values (see Ref. [5] for details). A very important fact is that the AM results *do not* predict the results of Juaristi *et al.* [2]. The reason is that the extension of the AM to account for BE is only applicable in the presence of an amorphous solid surface, more specifically when the atoms are at random. Juaristi *et al.* [2] calculated the bound probabilities with the quantum first Born approximation in the impact-parameter formalism, accounting properly for the planar channeling conditions.

By comparing the SLPA with the results of Juaristi *et al.* [2], we conclude that our approximation explains very well the main structure of the stopping. At the atomic surface, the SLPA yields a result very close to that obtained by Juaristi *et al.* [2]. Recall that they are quite different from the experimental values inside the solid, which are described properly

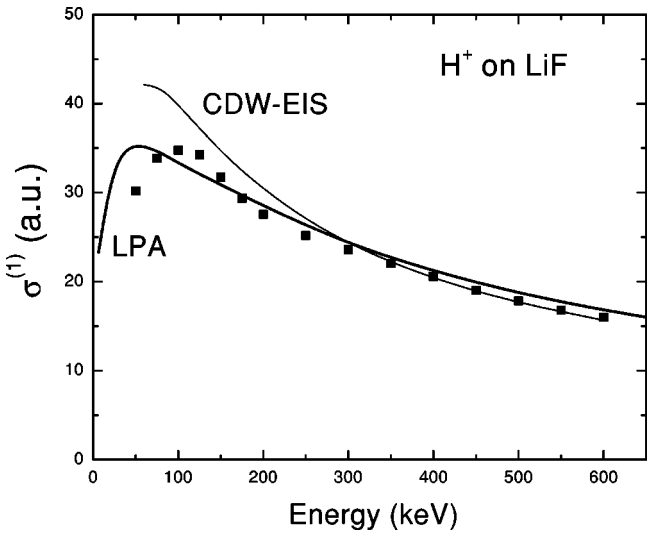

FIG. 2. Energy loss per atom in collision with solid LiF as a function of the incident proton energy. Notation: LPA and CDW-EIS approximation as indicated, and full symbols indicate the experiments of Ref. [19].

by the AM instead. The difference is that these experiments have been carried out with the atoms at random (beam-foil collisions) while here we use planar channeling.

B. Energy loss from lithium fluoride

First we investigate the capacity of the LPA to predict the data in the bulk. Stopping cross sections per atom $\sigma^{(1)}$ of protons on LiF are plotted in Fig. 2 and compared with the CDW-EIS calculation [18] and experiments [19]. The CDW-EIS is a distorted-wave method to calculate ionization amplitudes [20,21]. The agreement of the LPA with the experiments is excellent, at least at the level of integrated cross section.

Stoppings per unit path of 100 and 500 keV protons on LiF(100) surfaces are shown in Figs. 3 and 4, respectively, as a function of Z_0 due to the BE states $F^-(2s)$, $F^-(2p)$, and the total including $Li^+(1s)$ for 500 keV, which is not negligible. In these figures we also display the results of our calculation using the CDW-EIS under channeling conditions. In a recent paper we have used these CDW-EIS probabilities to calculate the track potential on LiF surfaces at 100-keV proton impact [18].

The BE wave functions were determined using the Hartree-Fok multiple *z* functions given by Clementi and Roetti [22]. For the (100) surface we find $\rho_{WS}=4.28$ differing substantially from $R_{WS}=3.74$. Just for the AM, the shifts of the edges with respect to the atomic surface were 1.25 for $F^-(2p)$, 1.03 for $F^-(2s)$, and 0.57 for $Li^+(1s)$. The effect of the inner shell $F^-(1s)$ was neglected. The SLPA fairly predicts the same value as the CDW-EIS for $F^-(2s)$, though it does not for $F^-(2p)$. The SLPA shows a different distribution but the same integrated value.

Although there is no FEG in this case, in Fig. 4(c), we also show the stopping probabilities by considering a *simile* FEG [23], as explained next. If we considered the F^- bound states as a FEG with an electronic density of 0.036 ($r_S=1.88$ or equivalent a volume plasmon energy $\omega=18$ eV), it would produce a stopping value per atom at 500 keV of 19 a.u., which coincides with the experimental result (see Fig. 1). This value of r_S does not differ largely from $r_S=1.5$ used by Sarasola *el al.* [23] to deal with low velocity ($v_i=0.5$) proton impact on LiF.

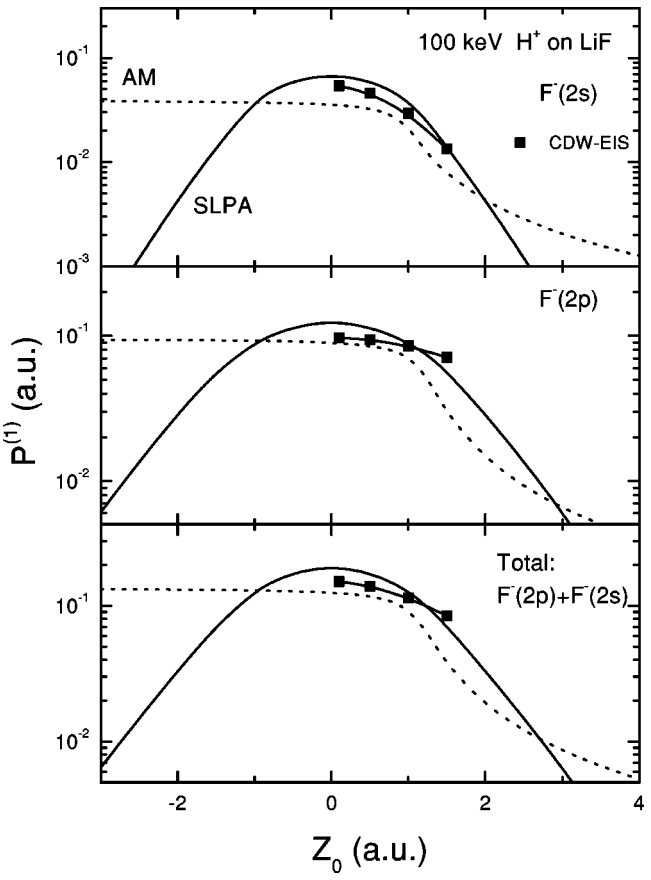

FIG. 3. Proton energy loss per unit length due to the bound states of LiF as a function of the distance to the atomic plane for 100-keV impinging energy. Notation: line plus full squares, results using the CDW-EIS; dotted lines, the axial model results; and solid lines, the surface local plasma approximation.

Note that the AM as well as the simile FEG are capable of describing the surface collective modes at large distances to the surface. The existence of the collective mode in the AM is guaranteed by the presence of factor $R(q,\omega)$. Spectrum distribution for the (volume and surface) collective modes for the FEG have been studied in Ref. [8]. There is a conceptual difference between the collective mode produced by the FEG and that produced by the BE that should be stressed. In the former, it is due to the well-known surface mode of free electrons found by Ritchie and Marusak [9], while in the latter the collective mode refers to the surface oscillation of the polarization of the bound states. Perhaps, the right word to define it would be *surface polaron*, but the definition of polaron was already introduced by Feyman in another context [24].

A major drawback of this SLPA is that it *does not* describe the surface collective mode at large distances from the surface because at distances $Z_0>\rho_{WS}$, the BE contribution van-

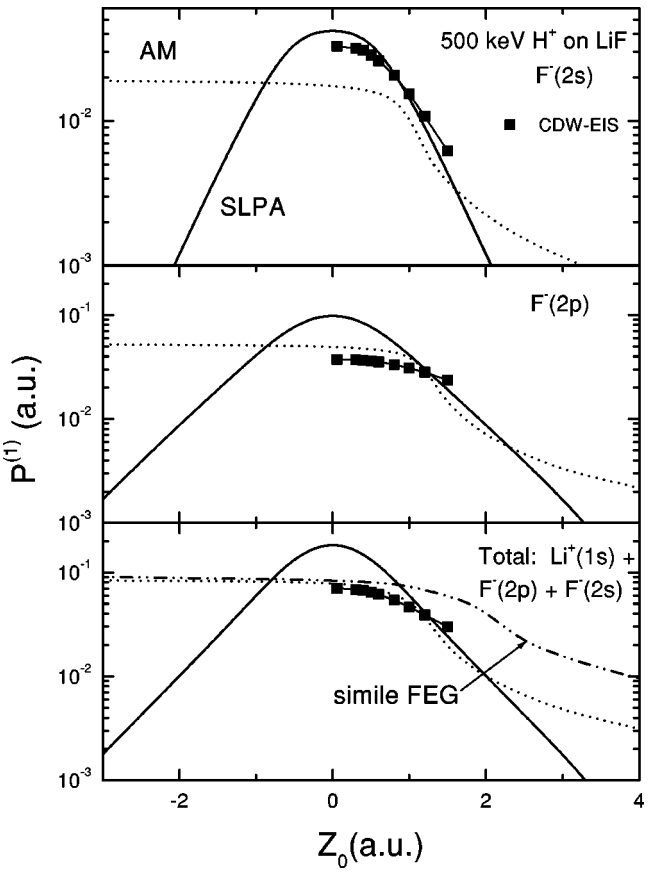

FIG. 4. Same as Fig. 3 for 500-keV impinging protons.

ishes completely in the restricted form. If $\Theta[\rho_{WS}-\rho]$ with $\rho=(Z_0^2+\rho^2)^{1/2}$ is dropped, the *unrestricted* form is used instead, probabilities at larger distances never vanish, although they decay very rapidly.

C. The induced potentials

There is one more feature of the AM that we would like to point out. The influence of the induced potential at the projectile position created by bound states is not negligible, as observed in Fig. 5. It is defined, in the usual way, as

$$V_{ind}(Z_0)=V_0\int_0^\infty d\omega\int_{\omega/v}^\infty\frac{dq}{q}\,\mathrm{Re}\left[\frac{1}{\varepsilon_{AM}(q,\omega,Z_0)}-1\right], \tag{12}$$

with $V_0=2Z_P/\pi v$. Bound-state polarization of the aluminum surface atoms accounts for a substantial contribution for $Z_0<0$ and rapidly vanishing for $Z_0>0$. This is a very important contribution if we analyze the survival of the bound states in solids [25].

In Fig. 5 we also plot the induced potential for 500-keV protons on LiF(100). Note that the polarization effect is very important, of the order of the FEG of aluminum, and so it should be included in the projectile trajectory. As a comparison, in Fig. 5 we also plot the induced potential created by the simile FEG, which is not very different from that produced by the AM.

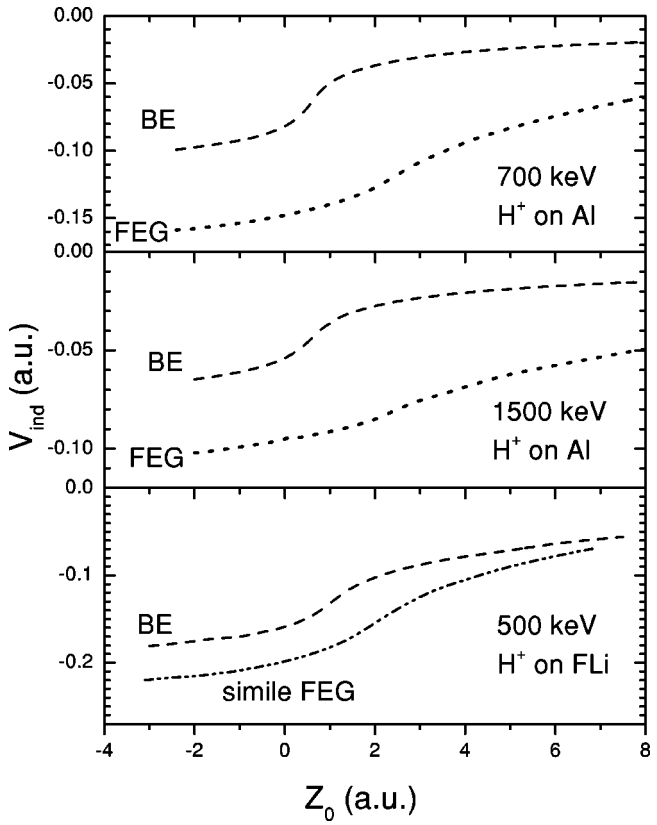

FIG. 5. Induced potential at the proton position calculated with the axial model for protons on Al and LiF as a function of the distance to the atomic plane. Surfaces and impact energies as indicated. The dashed lines labeled BE represent contributions of bound electron states, the dotted lines represent the FEG contribution, and the dash-double-dotted line represents the simile FEG calculation.

Note that we have considered here just the AM and not the SLPA to deal with IS. The reason is that the induced potential is a consequence of a sum of long-distance interactions, and a local approximation, such as the SLPA, would have no meaning.

IV. COMPARISON WITH THE EXPERIMENTS

In this section, we calculate total-energy loss S of protons incident on crystalline surfaces as a function of the incident angle ϕ_i. The total-energy loss is calculated in the usual form (see Ref. [1] for details)

$$S=2v\int_{Z_{\min}}^\infty\frac{P^{(1)}(Z)dZ}{\left[v^2\sin^2\phi_i-\frac{2}{M_P}U(Z)\right]^{1/2}}, \tag{13}$$

where $U(Z)=V_S(Z)+V_{si}(Z)$, $V_S(Z)$ is the proton-atomic surface potential (Ziegler-Biersack-Littmark [2] in our case) and $V_{si}(Z)$ is the self-induced potential. For the Al and SnTe cases, we restrict the calculation of $V_{si}(Z)$ to the response of the FEG alone calculated with the AM (which does not differ from the SRM as observed in Ref. [8]). We did not include the polarization of the BE states to comply with the standard

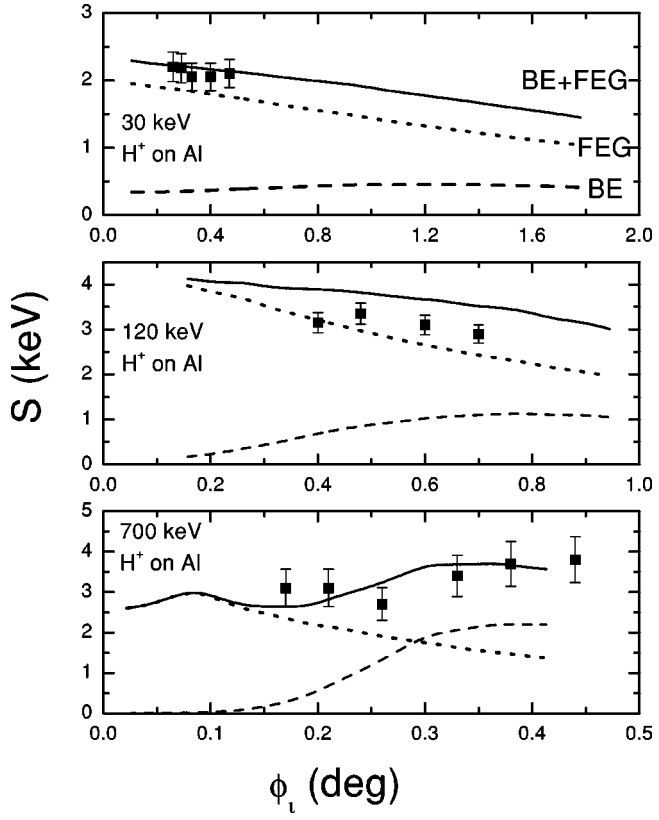

FIG. 6. Total-energy loss for protons colliding with Al(111) surfaces as a function of the incident angle in degrees. Impact proton energies as indicated. Theoretical results for bound electron states calculated with the SLPA and the FEG with the AM. Notation: dashed lines labeled BE represent bound electron states $(2p+2s)$ contributions, dotted lines show FEG, and solid lines show the total (sum) result. Symbols are the experiments of Winter *et al.* [27].

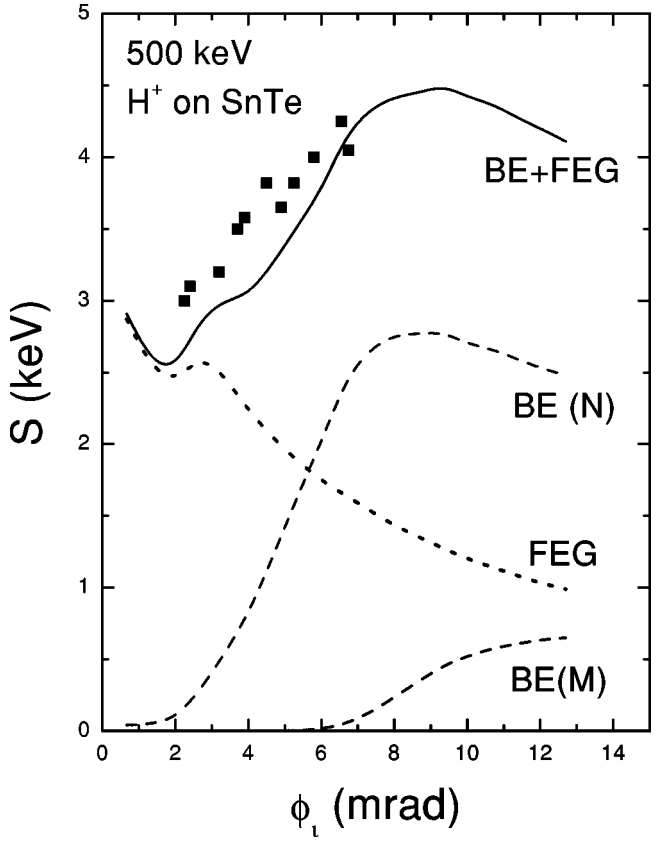

FIG. 7. Total-energy loss for 500-keV protons colliding with SnTe(100) surfaces as a function of the incident angle. Theoretical results for bound electron states are calculated with the SLPA and the FEG with the AM. Notation: dashed lines labeled BE show bound electron states for N $(n=4)$ and M $(n=3)$ contributions, dotted lines show FEG, and the solid line shows the total (sum) result. Symbols are the experiments of Kimura *et al.* [28].

procedure [2]. For the LiF case, we consider $V_{si}(Z)$ due to the polarization of the BE, as displayed in Fig. 4.

Total-energy losses for 30-, 120- and 700-keV protons on Al(111) surfaces are displayed in Fig. 6 as a function of the incident angle. To describe the response of the FEG we have used the Mermin-Lindhard function with a Fermi velocity $k_F=0.927$ (plasmon energy $\omega_p=0.582$) and a lifetime $\gamma=0.037$ [26]. The SLPA results are in very good agreement with the experiments of Winter *et al.* [27].

Total-energy losses for 500-keV protons on SnTe (100) surfaces are displayed in Fig. 7 as a function of ϕ_i and compared with the experimental data of Kimura *et al.* [28]. To describe the response of the FEG we have used the Mermin-Lindhard function with a Fermi velocity $k_F=0.746$ (plasmon energy $\omega_p=0.42$, it includes the $5s$ and $5p$ electrons of the O shell) and a lifetime $\gamma=0.313$ [29]. To represent the density of the BE states we have used the wave functions of Bunge *et al.* [17] for the antimony (nuclear charge 51), which averages Sn (50) and Te (52), and $\rho_{WS}=3.37$. Partial contributions of the FEG, M $(n=4)$ and N $(n=3)$ inner shells are also displayed in the Figure. Contribution of the L shell is negligible at this impact energy. Total-energy loss compares very well with the experiments of Kimura *et al.* [28]. This is the kind of targets that are liable to be described

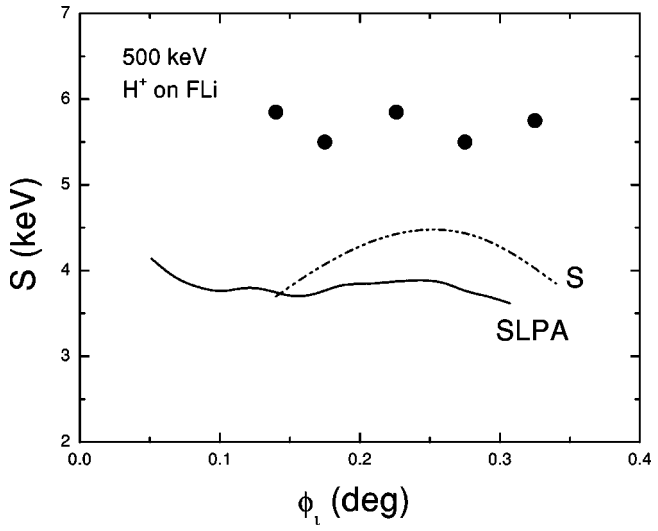

FIG. 8. Total-energy loss for 500-keV protons colliding with LiF(100) surfaces as a function of the incident angle. Notation: solid line, theoretical results calculated with the SLPA; the double-dot-dashed line labeled *S* shows results of Sarasola *et al.* [23]. Symbols are the experiments of Kimura *et al.* [30].

by the SLPA, i.e., where we have to deal with a large number of loose electrons (outer shells), something that makes the proper calculation nearly intractable and, for the same reason, the plasma description is more adequate. The more electrons, the better the SLPA should be.

Figure 8 shows energy loss of 500-keV protons on LiF (100) surface. The induced potential due to the polarization of the bound states, as displayed in Fig. 5, is here included to calculate the proton trajectory. The SLPA does not agree with the experiments [30]; it fails by a factor 2. Recent theoretical results reported by Sarasola *et al.* [23] run closely to ours and also disagree with the experiments. In principle, there is no reason to suspect the theoretical models unless there should be a *nonlocal* collective excitation [31]. To make sure that the failure is not due to the cutoff at ρ_{WS} introduced in the SLPA, we have considered a combined amplitude, i.e., for $Z_0<2$, the SLPA and for $Z_0>2$, the AM probabilities. In this way we have planar channeling probabilities at short distances from the surface, and the collective surface mode at large distances. Anyway, the result, not shown here, presents no increment.

V. CONCLUSIONS

We have studied the energy loss of protons colliding grazingly on metallic and insulator solid surfaces. To deal with projectiles moving parallel to surfaces of an amorphous solid, we have extended the AM, which guarantees the stopping of the bulk inside the solid and the presence of the surface collective mode at large distances from the surface. We found that the BE contributes substantially to the self-induced potential at the projectile position due to the polarization of the bound states.

If the surface, as in most of the cases, is characterized by a specific crystalline structure, we have found it appropriate to extend the LPA to account for planar channeling conditions. The model thus developed, which we call SLPA, agrees with previous calculations and explains the energy-loss experiments, except for the LiF case. The SLPA is designed to deal with surfaces of heavy atoms, such as SnTe, where the number of electrons makes the atomic collision calculation almost intractable on one hand, and, on the other, the loose electrons are more liable to be approximated by a plasma model.

ACKNOWLEDGMENTS

This work was supported by Grant Nos. PICT99 0303249, PICT98 0303579, and UBACyT X044. We are indebted to A. Arnau for his illuminating comments.

[1] J. Burgdörfer, in *Progress in Atomic and Molecular Phyisics*, edited by C.D. Lin (World Scientific, Singapore, 1993), and references therein.
[2] J.I. Juaristi, F.J. García de Abajo, and P.M. Echenique, Phys. Rev. B **53**, 13 839 (1996).
[3] J. Lindhard and M. Sharff, K. Dan. Vidensk. Selsk. Mat. Fys. Medd. **27**, 15 (1953).
[4] E. Bonderup, K. Dan. Vidensk. Selsk. Mat. Fys. Medd. **35**, 17 (1967).
[5] C. Montanari, J.E. Miraglia, and N. Arista, Phys. Rev. A **66**, 042902 (2002).
[6] J.D. Fuhr, V.H. Ponce, F.J. García de Abajo, and P.M. Echenique, Phys. Rev. B **57**, 9329 (1998).
[7] A. Sarasola, J.D. Fuhr, V.H. Ponce, and A. Arnau, Nucl. Instrum. Methods Phys. Res. B **182**, 67 (2001).
[8] J.E. Miraglia and M.S. Gravielle, Phys. Rev. A **66**, 032901 (2002).
[9] R.H. Ritchie and A.L. Marusak, Surf. Sci. **4**, 234 (1966).
[10] R. Nuñez, P.M. Echenique, and R.H. Ritchie, J. Phys. C **13**, 4229 (1980).
[11] F. Flores and García Moliner, J. Phys. C **12**, 907 (1979).
[12] J. Heinrichs, Phys. Rev. B **8**, 1346 (1973).
[13] J.L. Gervasoni, doctoral thesis, Universidad Nacional de Cuyo, 1992 (unpublished).
[14] A. García-Lekue and J.E. Pitarke, Phys. Rev. B **64**, 035423 (2001).
[15] J. Lindhard, K. Dan. Vidensk. Selsk. Mat. Fys. Medd. **28**, 8 (1954).
[16] D. Mermin, Phys. Rev. B **1**, 2362 (1970).
[17] C.F. Bunge, J.A. Barrientos, and A.V. Bunge, At. Data Nucl. Data Tables **53**, 113 (1993).
[18] A. Arnau, M.S. Gravielle, J.E. Miraglia, and V.H. Ponce Phys. Rev. A (to be published).
[19] M. Bader, R.E. Pixley, F.S. Mozer, and W. Whaling, Phys. Rev. **32**, 103 (1956).
[20] D.S.F. Crothers and J.F. McCann, J. Phys. B **16**, 3229 (1983).
[21] L. Gulyás, P. Fainstein, and A. Salin, J. Phys. B **28**, 245 (1995).
[22] E. Clementi and C. Roetti, At. Data Nucl. Data Tables **14**, 1177 (1974). Tables 2 (for Li^+) and 44 (for F^-).
[23] A. Sarasola, V.H. Ponce, and A. Arnau, Nucl. Instrum. Methods. Phys. Res. B (to be published).
[24] R. Feyman and A.R. Hibbs, *Quantum Mechanics and Path Integrals* (McGraw-Hill, New York, 1965).
[25] C.C. Montanari, J.E. Miraglia, and N. Arista, Phys. Rev. A **62**, 052902 (2000).
[26] N. Arista, Phys. Rev. A **49**, 1885 (1994).
[27] H. Winter, M. Wilke, and M. Bergomaz, Nucl. Instrum. Methods Phys. Res. B **125**, 124 (1997).
[28] K. Kimura, H. Kurada, M. Fritz, and M. Mannami, Nucl. Instrum. Methods Phys. Res. B **100**, 356 (1995).
[29] C. O. Reinhold (private communication).
[30] K. Kimura, G. Andou, and K. Nakajima, Nucl. Instrum. Methods Phys. Res. B **164-165**, 933 (2000).
[31] A. Arnau (private communication).